

Research Report 93
Tutkimusraportti 93

DETECTION OF IRREGULARITIES IN REGULAR DOT PATTERNS

**A. Sadovnikov, J. Vartiainen, J.-K. Kämäräinen, L. Lensu,
H. Kälviäinen**

Lappeenranta University of Technology
Department of Information Technology
P.O. Box 20
FIN-53851 Lappeenranta

ISBN 952-214-009-0
ISSN 0783-8069

Lappeenranta 2005

Detection of Irregularities in Regular Dot Patterns

A. Sadovnikov, J. Vartiainen, J.-K. Kamarainen, L. Lensu, H. Kälviäinen
Department of Information Technology,
Lappeenranta University of Technology,
P.O.Box 20, FI-53851 Lappeenranta, Finland

Abstract

Raster and halftone images are typically generated using small image elements, dots, which are organized and generated into a periodic structure to reproduce desired imaging effect. In this study, a periodic image element structure, referred to as a regular dot pattern, is defined, and based on the definition, two methods are introduced to detect irregularities in regular dot patterns. An example application for the methods is an automatic assessment of Heliotest sample prints. Heliotest assessment is used in the paper and printing industry to measure printability of different paper grades. In the experimental part the proposed methods are applied to detect missing elements, dots, from digitized Heliotest samples which are considered to form a regular dot pattern.

1 Introduction

In this study, by regular dot patterns it is referred to images which contain similar dots of a same color and the spatial spacing between dots is regular. Local dot presentations, their shape and color, and spatial spacing of dots may vary, but the variation should be substantially small over the whole image. Thus, locations where features deviate significantly from the normal variation are considered as irregular. One of the most typical application area where regular dot patterns would be present is halftone imaging (e.g., [7]). Correspondingly, a method for an accurate detection of dot pattern irregularities would be useful in the quality control of halftone printing, for example, to find the number of missing dots in rotogravure prints [11]. The main motivation for this work is a quality assessment known as Heliotest paper printability test in the paper and printing industry. Heliotest is recognized as a standard quality assessment and it is currently performed manually by laboratory experts. However, a modern industrial environment sets new quality standards and there is an increasing demand for reliable process and quality control automation. That is the main reason why there is common interest in paper and printing companies to develop an accurate and reproducible missing dot detection method.

An image processing sub-field which contains the most similar characteristics with regular dot patterns is evidently textures and texture analysis. However, in texture analysis the most typical problem is to distinguish between different types of textures, and thus, proposed approaches favor between-texture type of processing while in irregularity detection a within-texture type of processing is needed. Still, there are many proposed texture characteristics and notations which can be used, i.e., dots can be considered as texture atoms and the dot spacing can be represented as spatial interrela-

tionships between atoms [5]. Related research to regular dot patterns and irregularity detection have been done also in fabric defect detection [4], but the given problem setting is also too simple for missing dot detection: fabric defect detection is concerned about “Where is something wrong within the given texture”, but in addition to that it is necessary to find “What is wrong in the given location”. In other words, one needs to find both locations where there are irregularities, i.e., local dot presentation fails, and what kind of irregularities they are, a partly or completely missing dot or a group of dots. Several image processing methods for missing dot detection have been proposed, e.g., by Langinmaa [8] and Heeschen and Smith [6], but their accuracy cannot meet industrial requirements.

In this study, a more comprehensive treatment is given to regular dot patterns and to the irregularity detection from them. The regular dot patterns are first defined and based on the definition two methods are proposed for an accurate irregularity detection. In the experimental part the proposed methods are applied to missing dot detection from rotogravure test strips (Heliotest) strips where the methods provide detection accuracies sufficient for the industrial use.

2 Regular dot patterns

It is worthwhile to define terms dot and pattern in this context. A dot is a particular type of a texture atom; an indivisible atom which can be represented for example by 2-d Gaussian function. A pattern is a set of spatial coordinates, in which dots are reproduced. When the pattern expresses some degree of periodicity it can be considered as regular. Similar definitions and results are used in solid state physics and especially in definitions of crystal lattice structures [1].

2.1 Pattern regularity

Regularity is a property which means that some mnemonic instances follow predefined rules. In the spatial domain regularity typically means that a pattern consists of a periodic or quasi-periodic structure of smaller pattern units or atoms, and thus, it is worthwhile to explore pattern regularity in terms of periodical functions and especially via their Fourier transforms. The following is mainly based on definitions in solid state physics and is related to Bravais lattice formulations: A Bravais lattice is an infinite array of discrete points with an arrangement and orientation that appears exactly the same, from whichever of the points the array is viewed. A two-dimensional (2-d) Bravais lattice consists of all points with position vectors \mathbf{R} of the form

$$\mathbf{R} = n_1\vec{a}_1 + n_2\vec{a}_2 \quad (1)$$

where \vec{a}_1 and \vec{a}_2 are any two vectors not both on the same line, and n_1 and n_2 range through all integer values. The vectors \vec{a}_i are called primitive vectors and are said to generate or span the lattice. It should be noted that the vectors \vec{a}_i are not unique. In Fig. 1 is shown a portion of a two-dimensional Bravais lattice. [1]

The definition of Bravais lattice refers to points, but it can also refer to a set of vectors which represent another structure. A point as an atom can also be replaced with any, preferably locally concentrated, structure. A region which includes exactly one lattice point is called a primitive unit cell and \vec{a}_i now define spatial relationship of unit cells. Unit cells can also be defined as non-primitive but in both cases they must

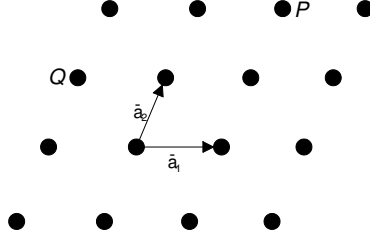


Figure 1: A two-dimensional Bravais lattice of no particular symmetry, an oblique net. All the net points are linear combinations of two primitive vectors (e.g. $P = \vec{a}_1 + 2\vec{a}_2$, and $Q = -\vec{a}_1 + \vec{a}_2$).

fill the space without any overlapping. The primitive and non-primitive unit cells are not unique. [1]

2.2 Fourier transform of 2-d periodic functions

Let us consider a function $f(\vec{r})$ (where $\vec{r} = (x, y)$) in which the spatial domain is a periodic extension of a unit cell. Periodicity can be formally described. Let M be a 2×2 matrix which is invertible and such that

$$f(M\vec{m} + \vec{r}) = f(\vec{r}) \quad (2)$$

where \vec{m} is any 2-dimensional integer vector. Now, clearly, every point \vec{r} in the space can be written uniquely as

$$\vec{r} = M(\vec{n} + \vec{u}) \quad (3)$$

where \vec{n} is a 2-dimensional integer vector and \vec{u} is a vector where each coordinate satisfies $0 \leq u_i < 1$. An unit cell $\mathcal{U}(M)$ is the region in space corresponding to all points $M\vec{u}$. It can be shown that the volume of unit cell is $V = |\det M|$.

The set of all points $\mathcal{L}(M)$ of the form $M\vec{n}$ is called the lattice induced by M . A point in the space corresponds a point in the unit cell translated by a lattice vector. Note that a sum of two lattice vectors is a lattice vector and the periodicity of function f implies that its value is invariant under translations by multiples of the lattice vector. A matrix \hat{M} can be obtained by inverting and transposing M

$$\hat{M} = M^{-T} \quad (4)$$

For \hat{M} new lattice and unit cell can be associated, called the reciprocal lattice $\mathcal{L}(\hat{M})$ and the reciprocal unit cell $\mathcal{U}(\hat{M})$, respectively. If we consider wave number space, each vector \vec{k} is written uniquely as

$$\vec{k} = \hat{M}(\vec{\kappa} + \vec{\xi}) \quad (5)$$

where $\vec{\kappa}$ is a 2-dimensional integer vector and $\vec{\xi}$ has all ordinates $0 \leq \xi_i < 1$. The reciprocal lattice vectors span the lattice points $\hat{M}\vec{\kappa}$.

The fundamental result is that the Fourier transform of a periodic function with a unit cell specified by M has a discrete spectrum, peaks located at the reciprocal lattice

points specified by \hat{M} [1]. That is, the wavenumber vectors are constrained to lie at the reciprocal lattice points. The explicit transform and inverse transform formulas are

$$\hat{f}_M(\vec{k}) = \frac{1}{|\det M|} \int_{\vec{r} \in \mathcal{U}(M)} f(\vec{r}) e^{-j(\vec{k} \cdot \vec{r})} dV(\vec{r}), \quad \vec{k} \in \mathcal{L}(\hat{M}) \quad (6)$$

and

$$f(\vec{r}) = \sum_{\vec{k} \in \mathcal{L}(\hat{M})} \hat{f}_M(\vec{k}) e^{j\vec{k} \cdot \vec{r}}. \quad (7)$$

The discrete spectrum can be interpreted as a continuous spectrum consisting of Dirac impulse functions located at the reciprocal lattice points

$$\hat{f}(\vec{k}) = \sum_{\vec{\kappa} \in \mathcal{Z}^D} \hat{f}_M(\hat{M}\vec{\kappa}) \delta(\vec{k} - \hat{M}\vec{\kappa}). \quad (8)$$

2.3 Fourier transform of 2-d quasi-periodic functions

In the general case we can take a 2-d image which is approximately periodic (quasi-periodic). Consider a pattern image whose unit cell and lattice structures are specified by M . If this image is unbounded in all directions, and we can consider a function which is periodic (i.e., invariant under translation by a lattice vector), then it is the superposition of waves whose wavenumber vectors are necessarily precisely lattice vectors in the reciprocal lattice, specified by $\hat{M} = M^{-T}$.

However, a real image has a finite extent and has imperfections (irregularities). The ideally periodic function is constrained to satisfy certain boundary conditions. We illustrate the consequences of this by considering the situation, where the pattern is comprised only a finite number of translates of the unit cell. Let \mathcal{V} denote the finite region occupied by the pattern, and consider the window function $w_{\mathcal{V}}(\vec{r})$ defined as

$$w_{\mathcal{V}}(\vec{r}) = \begin{cases} 1, & \vec{r} \in \mathcal{V} \\ 0, & \text{otherwise} \end{cases} \quad (9)$$

If $f(\vec{r})$ is the ideal, truly periodic function (with periodicity specified by M) and $f_{\mathcal{V}}(\vec{r})$ is the truncated function

$$f_{\mathcal{V}}(\vec{r}) = w_{\mathcal{V}}(\vec{r}) f(\vec{r}) = \begin{cases} f(\vec{r}), & \vec{r} \in \mathcal{V} \\ 0, & \text{otherwise} \end{cases} \quad (10)$$

then $f_{\mathcal{V}}(\vec{r})$ has a continuous spectrum given by

$$\hat{f}_{\mathcal{V}}(\vec{k}) = \sum_{\vec{\kappa} \in \mathcal{Z}^3} \hat{f}_M(\hat{M}\vec{\kappa}) \hat{w}_{\mathcal{V}}(\vec{k} - \hat{M}\vec{\kappa}) \quad (11)$$

where $\hat{w}_{\mathcal{V}}$ is the Fourier transform of $w_{\mathcal{V}}$.

It can be shown that $\hat{w}_{\mathcal{V}}$ contains a continuous spectrum which has infinite extent, but which fades out proportionately fast with $1/|\vec{k}|$.

The most important result is that quasi-periodic functions have quasi-discrete spectra, with the spectral energy concentrated at points in the reciprocal lattice.

2.4 Pattern irregularity

In terms of function periodicity, pattern irregularity can be defined as an aperiodic function $\varepsilon(x, y)$, with spatial energy $|\varepsilon| \ll |f_V|$.

Finally, the initial 2-d pattern image can be represented as

$$f_V(\vec{r}) = w_V(\vec{r}) f(\vec{r}) + \varepsilon(\vec{r}) \quad (12)$$

and the problem is to separate the regular part $w_V(\vec{r}) f(\vec{r})$ and the irregular part $\varepsilon(\vec{r})$ as accurately as possible.

3 Extracting regular pattern information

As it was described in the previous section the formation of model of the ideal regular part of an image is crucial for the irregularity detection; the more accurate model can be established the more accurate detection and classification of irregularities can be made.

The details level needed for the regular part formation is particularly high for example in Heliotest images [12], and thus, typical texture segmentation methods (e.g. [5]) or defect detection methods (e.g. [4]) cannot provide a sufficient accuracy.

One attractive approach to estimate an ideal regular pattern is to form an analytical model and to estimate model parameters based on an input image. This approach has been proposed for example in [4], but this requires a correct and very accurate analytical model, in which case, the parameter estimation may become very unstable and slow. Typically real images do not correspond any analytical models but they contain distortions and noise. Due to these facts it is motivated to use the analytical model only as a restricting bias in the regular pattern formation and allow incompleteness by extracting the regular pattern from an input image itself. This approach has been applied in the frequency domain self-filtering to emphasize regular patterns [2] and will be the case in the approaches proposed in this study as well. Results from the regular lattices and the reciprocal lattice are applied, but only to estimate appropriate model parameters while details are extracted from an input image. What affects to the selection of this approach will be discussed next.

3.1 Spatial modeling limits of accuracy

Before it is proposed how to extract the ideal regular pattern from an input image it is important to explain why all parameters of the analytical model cannot be directly estimated. Different kind of analytical models would be the most obvious solutions since they are commonly used in a regular dot pattern synthesis, e.g., in digital halftoning [7], and also used in defect detection (e.g. [4]). In the context of regular dot patterns the analytical expression in (12) can be used, but the limits of accuracy prevent to estimate the model parameters directly; practical restrictions due to the discrete image resolution which cannot be bypassed. For the same reason, the limited available resolution, a halftone synthesis is not necessarily reversible.

In Fig. 2(a) is shown a simplified model of regular dot patterns which can also be used to describe the pattern in Heliotest assessment [11, 12]. Parameters of the model can be divided in the following classes:

1. Image geometry parameters, i.e., lattice primitive vectors \vec{a}_1, \vec{a}_2 (see Fig 2(a)) and overall lattice shift vector \vec{s} .

2. Unit cell model parameters. For example, in the case of Heliotest it can be a 2-d Gaussian hat (see Fig 2(b)).

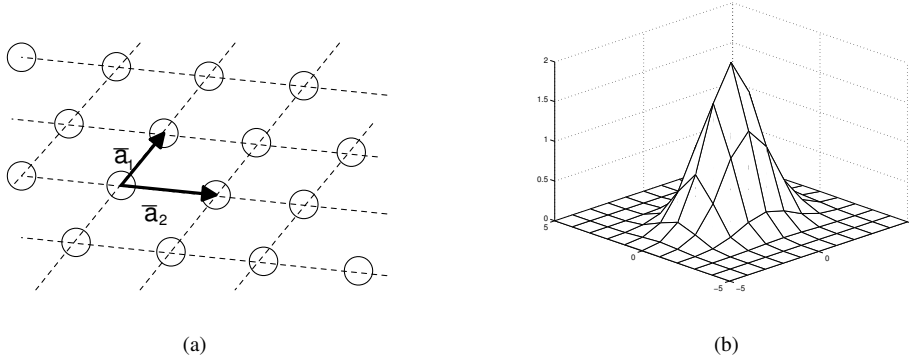


Figure 2: Simple model of regular dot pattern (Heliotest): (a) 2-d lattice structure (\vec{a}_1, \vec{a}_2 - primitive vectors); (b) Gaussian dot model (μ, Σ, A).

The estimation of all above-mentioned parameters is necessary in order to generate an accurate ideal regular pattern which can be used in irregularity detection by comparing or subtracting it from the observed image. However, the estimation is not trivial; it can be performed with search or generic optimization methods where a target function to be minimized is for example energy difference between observed image and model. Unfortunately the number of optimized parameters is very high and they cannot be independently optimized.

The first step in the pattern modeling is estimation of the lattice parameters (\vec{a}_1, \vec{a}_2) representing periodicity (lattice matrix M). These parameters can be derived using a number of techniques: using image autocorrelation space, image texture statistics (gray-level statistics), LBP (local binary pattern), fixed window features, etc. During periodicity estimation some problems may arise, such as incorrect period estimation (convergence to harmonics nM instead of M). A solution for the periodicity ambiguity is a correct initial period guess. For example, in Heliotest proper limits of search domain for vectors \vec{a}_1, \vec{a}_2 must be defined. This approach depends on the input image and further generalization seems to be of a low success.

Based on the statistics, it is possible to derive estimation parameters: mean lattice matrix M_μ and lattice matrix deviation M_Σ over the statistics. The question arises, if the mean lattice matrix can be used as a model of the ideal lattice. Unfortunately, practical experiments showed that it cannot; the observed lattice from an input image is not typically regular enough but it should be modeled rather as a real world stochastic process. The only possible way of using this modeling approach would be a local refining where each lattice grid point is adjusted to a corresponding unit cell in observed image. This in turn will cause additional computational expenses which prevent an efficient implementation of the method. Furthermore, additional model parameters introduce more uncertainty and more adjustment is required.

It is evident that it is easy to construct a mathematical model to synthesize regular dot patterns, but this process is often irreversible in practice due to the limited acquisition resolution and exhaustive computation needed in the parameter estimation. With

the help of application specific heuristics, a combination of direct estimations and optimization may still succeed, but whether that is accurate and computationally feasible is questionable and thus an alternative approach is needed.

3.2 Exploiting Fourier domain

Let us now consider real images which represent regular dot patterns. Such images are produced by the Heliotest assessment as shown on the left-hand-side in Fig. 3. Let us next consider Fourier spectra of the given image, i.e., the magnitude spectra. On the right-hand-side in Fig. 3 it is possible to see the distinctive frequency peaks which in turn are located at the reciprocal lattice points in (6).

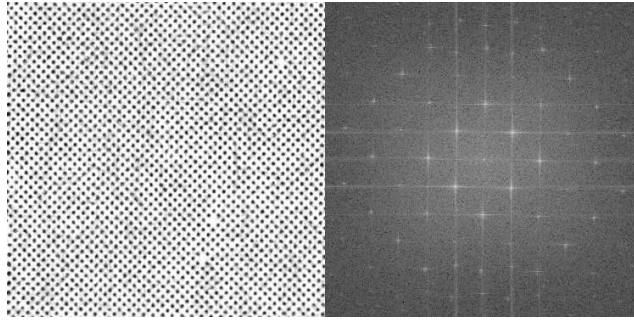


Figure 3: Example of regular dot pattern image (Heliotest) and its Fourier spectra magnitude.

It is clear that by filtering out the reciprocal lattice frequencies it is possible to estimate the faultless periodic component, the ideal regular pattern, of the input image and utilizing it also the defect component, irregular part. These two parts are now called as the regular and irregular parts of the image and demonstrated in Fig. 4, respectively. The separation of the parts can be formulated as

$$\begin{aligned}
 \xi(x, y) &= \mathfrak{F}^{-1}\{\Xi(u, v)\} = \\
 &= \mathfrak{F}^{-1}\{\mathfrak{M}(u, v)\Xi(u, v) + (I(u, v) - \mathfrak{M}(u, v))\Xi(u, v)\} = \\
 &= \mathfrak{F}^{-1}\{\mathfrak{M}(u, v)\Xi(u, v)\} + \mathfrak{F}^{-1}\{(I(u, v) - \mathfrak{M}(u, v))\Xi(u, v)\}
 \end{aligned} \tag{13}$$

where $\xi(x, y)$ is the spatial image, \mathfrak{F} and \mathfrak{F}^{-1} are forward and inverse discrete Fourier transforms, $\mathfrak{M}(u, v)$ is a mask filter (real valued function of the same definition domain as $\Xi(u, v)$), and $I(x, y)$ is a unit function. The decomposition in Eq. (13) is possible according to identity of the addition operation in the spatial and frequency domains. The mask filter can be of any type, suitable for a particular application, i.e., accept/reject (binary), notch filter, etc. The only condition for the mask is that it should remove periodic component while preserving other frequencies unchanged, i.e., it should have band-pass on frequencies near the reciprocal peak points.

3.3 Spatial domain vs. Frequency domain

Many image processing techniques work well directly in the spatial domain. However, when it comes to the repetitive patterns the choice of frequency domain is obvious. Due

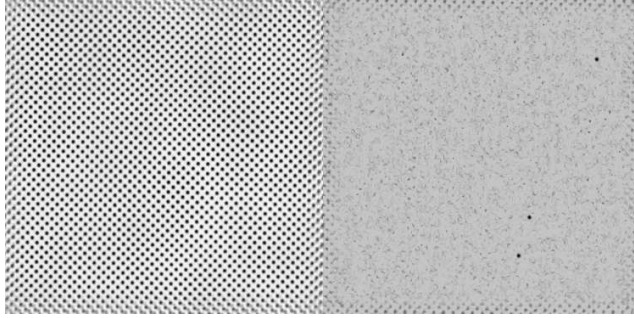


Figure 4: Examples of regular and irregular image parts (Heliotest).

to the FFT algorithm, forward and inverse Fourier transforms can be made efficiently fast. 2-d periodicity in the spatial domain is given by a lattice matrix M and a 2-d periodic function in the frequency domain has a discrete spectra located at the reciprocal lattice M^{-T} points. For an $N \times N$ image the FFT transform is also $N \times N$ with discrete frequencies ranging from 0 to $(N - 1)/N$ (wave numbers $0, \dots, N - 1$). If the input image pattern contains a large number of unit cell translations, the frequency picture will be sparse having a small number of lattice points in it. The conclusion is that a rough estimation of lattice matrix M through a reciprocal matrix M^{-T} is easier.

However, inspecting small details, such as the shape of a single unit cell, is a difficult task in the Fourier domain, and respectively the inverse transform back to the spatial domain is needed in a detailed analysis. These issues will be discussed next in the description of algorithms we propose.

4 Irregularity detection algorithms

In this section, two different algorithms are proposed to detect irregularities in regular dot patterns. The description is quite thorough, though presented in a more practical way. Before proceeding to the actual methods, it needs to be said that presented algorithms are aimed at the detection of missing dots in 2-d periodic dot patterns.

4.1 Method based on Fourier domain regularity detection and global gray-level processing in the spatial domain

This method (referred to as method 1) is based on the fact that the periodic regular structure provides intensity peaks in the Fourier domain as demonstrated for the periodic function f and its reciprocal counterpart \hat{f} in Eqs. (2) and (8). If the mask \mathfrak{M} can be automatically generated by utilizing locations of the peaks in the frequency domain regular and irregular parts of an image can be extracted using Eq. (13). From an irregular image it is possible to find irregularities by global processing; by thresholding a gray-level irregular image and processing the resulting binary areas (see the right-hand-side in Fig. 3). The following stages are needed:

1. Image preprocessing to eliminate illumination changes and acquisition noise.

2. Extracting the irregular component by forming the mask based on the peak frequencies.
3. Global processing of the irregular image part.

These processing steps will be considered next.

4.1.1 Image preprocessing

At first, if the observed image is very noisy, the noise magnifies energy of the irregular component, and thus, it is possible to achieve better results by denoising the image in advance. Denoising can be performed using standard approaches, such as median, average, or low-pass filtering (e.g. [3]).

In the following it is assumed that the dots forming the regular pattern are represented by high gray-level intensity values and background corresponds low gray-level intensity values. Furthermore, the values are assumed to be normalized to $[0, 1]$ (minimum value subtracted and then normalized by the maximum).

4.1.2 Irregular component extraction

A general approach for irregular component extraction was established by introducing the theory of reciprocal lattices of periodic patterns in Section 2 and by the separation principle in Section 3.2. The extraction is described in Algorithm 1.

Algorithm 1 *Irregular image extraction*

- 1: *Compute magnitude of the Fourier transform $|\Xi|$ of an input image ξ .*
- 2: *Form the reciprocal lattice vectors using locations of magnitude peaks.*
- 3: *Create the mask \mathfrak{M} by setting Gaussian band-pass filters to reciprocal lattice points.*
- 4: *Extract the irregular component from ξ using the mask \mathfrak{M} and the inverse Fourier transform.*

The first and last steps are clear enough, but the other two need a more detailed description. The second step actually introduces a dual problem corresponding to the title of this study: detection of the regularity in regular dot patterns. The reciprocal lattice is defined by the primitive vectors, which can be estimated within a sub-pixel accuracy using the peak locations, but estimation may be sensitive to the initial guess. The estimation ambiguity occurs due to harmonic components and can only be prevented using a sufficiently accurate initial guess. Another ad hoc solution would be to locate all frequency peaks, but since the frequency plane is discrete, the harmonic set estimation based on lower frequencies is not accurate and they need to be adjusted to actual local maxima. This adjustment is performed by looking for a local maximum in a certain neighborhood. This neighborhood can be defined as a rectangular area with the first approximation point in the center and should contain only one local maximum from the harmonics set.

The filter mask generation is based on the reciprocal lattice and a band-pass filter suitable for an application (in Heliotest Gaussian band-pass filters are used). Two image components are derived from the observed image, one containing regular image part and the other containing irregular.

4.1.3 Processing irregular image

The irregular image produced by Algorithm 1 must be further processed to locate which irregularities are significant for the detection. The irregular image may still contain noise, which can be removed using standard noise removal methods, and then, processing of the irregular image can be defined according to Algorithm 2

Algorithm 2 *Detecting irregularities from irregular image*

- 1: *Threshold the irregular image ξ_I using the threshold limit τ .*
- 2: *Remove foreground areas of a size less than S .*
- 3: *Compute centers of each foreground areas.*
- 4: *Return centers as irregularity coordinates.*

There are various methods which can be used to perform the binary processing tasks in Steps 2 and 3, e.g., areas less than S can be removed using the binary opening procedure [3]. Algorithm 2 requires two parameters to be defined: a threshold value τ and the minimum area S . Due to image normalization in the previous stages a fixed threshold values can be used. These values can also be estimated using a training set.

4.2 Method based on Fourier domain regularity detection and local gray-level processing in the spatial domain

This approach (referred to as method 2) can be divided into:

1. Regular spatial lattice points estimation.
2. Local classification at spatial lattice points.

4.2.1 Spatial lattice estimation

Spatial lattice estimation correspond to the estimation of irregularities in the regular part, and thus, Algorithms 1 and 2 can also be used to find centroids of the unit cells. The only difference is that the regular image part is used instead of the irregular one. When all the centroids of the regular image part are located the original image can be processed and analyzed at each unit cell location.

4.2.2 Local classification at spatial lattice points

The locations of the unit cells were extracted using the regular image and next the decision can be made at the each location in order to make the decision if it is regular or irregular, not missing or missing (see Fig. 5). First, some kind of feature extraction is needed, e.g., simply the vector of all gray-level values. After feature extraction they can be classified using a classifier. There is a vast amount of applicable methods available and for vectors of gray-level values a principal component subspace classifier can be used [10]. It should be noted that in this approach a separate training set is needed, but the local processing approach also provides detailed information about the type of missing dots.

5 Experiments

In the experiments, the methods and algorithms are applied to real data.



Figure 5: Examples of dots in Heliotest images: (a)-(c) Regular dots; (d) Regular dot expectation; (e)-(g) Missing dots; (h) Missing dot expectation (note that not completely missing).

5.1 Heliotest data

Paper printability is a property which describes how a certain paper type behaves in printing process. In general, the printability property depends on interactions between paper and printing ink, and variables of printing process itself. Good printability generally means that the paper is not sensitive to variations in the variables and provides good print quality. Thus printability describes the final result of printed images. It is clear that print quality does not have absolute terms, but it depends on many factors, such as the print density, resolution, and evenness of the printed image. In practice, an estimation of the print quality can be generated based on several different quality assessments. [9]

In rotogravure printing process, the greatest difficulties involve in reproduction of light and medium tones. In the reproduction of tones, the two recognized defects are missing dots and waving. In the missing dot defect, the ink is not transferred to the paper which is considered to be due to a bad quality of paper. Paper surface does not allow the ink to soak into the paper. Missing dots are inevitable at 5% half tone, but disastrous when occurring at 20% and 30% half tones [9]. Half tone means a tone which is in between the paper color and the ink color. A specific half tone can be generated by transferring a corresponding amount of ink. In dark areas (close to ink color), missing dots are more visible. Now, it is evident why the number of missing dots in an image area is a traditional measure of the rotogravure printability of paper. To measure the number of missing dots the test assessment Heliotest was developed and standardized for laboratory printing by the Centre Technique du Papier (<http://www.webctp.com>).

A rotogravure print sample is generated using a special Heliotest device and the assessment itself, i.e., the counting of missing dots, is performed by visual inspection. The sample strip contains a printed dot pattern (Fig. 6(a)) which may have some of the dots missing (Fig. 6(b)). Furthermore, as it can be seen in Fig. 6(a), color gradually

changes lighter along the strip which is due to a smaller dot size in the rotogravure cylinder (less ink).



(a)



(b)

Figure 6: Heliotest strips: (a) Example of a typical Heliotest strip, the dimensions of the region of interest are 110mm by 85mm; (b) Part of the strip magnified.

5.1.1 Measuring performance

The manual assessment introduces variance to the quality and thus, an automatic assessment method would be beneficial for the laboratories of the paper and printing industry [12]. The Heliotest dot pattern forms a visual structure which has been considered as the regular dot pattern in this study. Thus, a method for an accurate irregularity detection could be used to detect the missing dots as well.

For the experiments, a set of reproduced Heliotest strips were scanned using 1200 dpi resolution. The training set consisted of 75 images and the test set of 70 images. The training set was needed to train set of the two classes: a dot and a missing dot, in the method described in Section 4.2.2. In addition, as it was mentioned the parameters of the rotogravure cylinder change along the strip, i.e., ink cups are smaller, and respectively, the dots become smaller and lighter. Thus, the strip was processed as separate windows which had their own parameter values in irregularity detection. For the selection of parameter values the training set images were used.

Since the ground truth for missing dots was carefully created by visually inspecting the printed strips, the comparison was done with respect to the manual selections. At first, a radius from the ground truth points was defined and if within a specific distance there was also an automatically detected missing dot, the corresponding missing dot was considered to be detected. Similarly, all automatically detected dots which were outside the specific radius were considered as false alarms.

A more descriptive measure comes directly from the industry: the distance from the beginning of the strip to the 20th missing dot.

5.1.2 Results

The results are reported for the proposed methods, global processing of irregular image (Method 1) and local processing of original image (Method 2).

The number of detected missing dots and false alarms as functions of radius from the ground truth missing dots are shown in Fig. 7 for the both methods. From the figure it can be seen that the local processing (Method 2) provides more accurately detected missing dots within a distance and less false alarms. The results are demonstrated in pixels while the mean shortest distance between two dots was 7.1 pixels and the graphs in Fig. 7 end at 4.0 pixels.

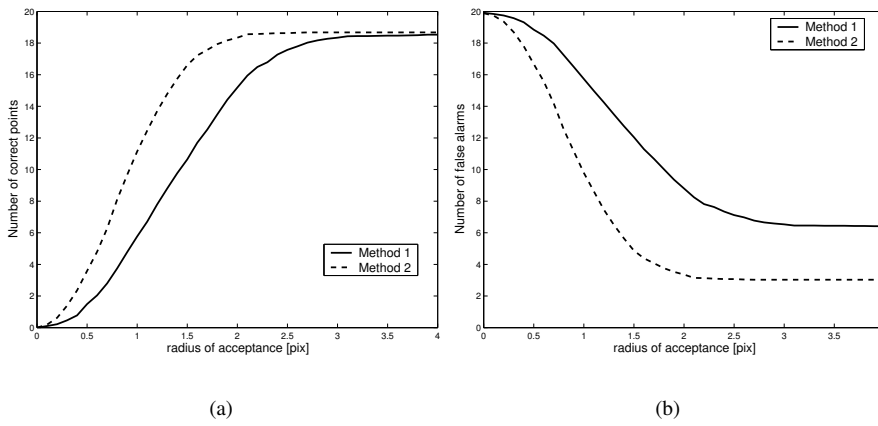


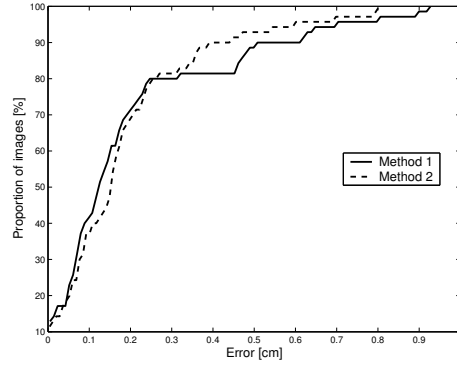
Figure 7: Detection accuracy as a function of radius from the ground truths for the both methods: (a) Correctly detected missing dots; (b) False alarms.

A more meaningful measure is the distance to the 20th missing dot which is the measure used in the industry. Figure 8. shows the accuracies for the both methods as compared to the ground truth distances to the 20th missing dot. Method 2 outperforms Method 1, and for 90 per cent of images the distance is within 5.0 *mm* of the actual location. The error distribution for the both methods are shown in Figs. 8(b) and 8(c). The mean absolute error for Method 1 was 2.0 *mm* and for Method 2 1.9 *mm*

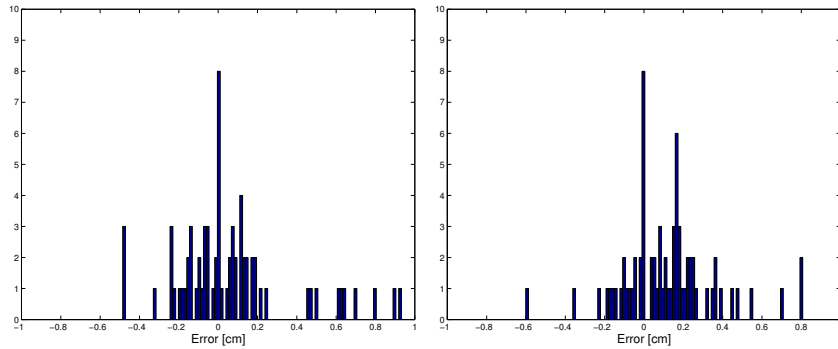
6 Conclusions

In this study, the regular dot patterns were defined. The regularity was defined by using the 2-d periodicity of the pattern where the repeated shape, the unit cell, was considered to be dot shaped. However, the given results hold for any given unit cells, but the proposed irregularity detection methods may fail for other than convex unit cell entities (dots).

Based on the results on periodic lattices and their reciprocals, two methods were proposed to accurately detect irregularities in regular dot patterns, i.e., completely or partly missing unit cell entities. The both methods assume that image can be divided into a regular part and to an irregular part where the regular part is sufficiently strong to be detected in the reciprocal space. The first method directly utilizes the irregular part



(a)



(b)

(c)

Figure 8: Accuracy of distances to the 20th missing dot as compared to the ground truth: (a) Percentage of images where specific accuracy was achieved; (b) Error histogram for the global processing; (c) Error histogram for the local processing.

and processes it globally to detect the most visible irregularities. The second method utilizes the regular part to find the centroids of all unit cells (convexity requirement) and then locally distinguishes whether a cell is distorted or not by using a classifier.

In the experimental part of this study, the proposed methods were applied to detect missing dots from digitized Heliotest images, and both achieved an accuracy of less than one centimeter. The mean values were approximately 0.2 mm in the detection of 20th missing dot which is an acceptable error rate in the industry.

Any analytical solution to solve the reciprocal lattice matrix directly, and respectively, to estimate the lattice matrix was neglected due to the claimed lack of accuracy in the discrete representation. However, there are techniques which may still allow direct estimation and very efficient detection of the lattice matrix. Then a global or local processing and convexity requirements are not needed anymore, but the unit cells can be detected also automatically providing a more general description of regular patterns and irregularity detection. This issue will be addressed in the future work.

References

- [1] Neil W. Ashcroft and N. David Mermin. *Solid State Physics*. Thomson Learning, Inc., 1976.
- [2] D.G. Bailey. Detecting regular patterns using frequency domain self-filtering. In *Proc. Int. Conf. on Image Processing*, volume 1, pages 440–443, Washington DC, USA, 1997.
- [3] R. C. Gonzalez and R. E. Woods. *Digital Image Processing*. Prentice-Hall, Inc., 2002.
- [4] C. h. Chan and G.K.H. Pang. Fabric defect detection by Fourier analysis. *IEEE Trans. on Industry Applications*, 36(5):1267–1276, 2000.
- [5] Robert M. Haralick. Statistical and structural approaches to texture. *Proc. of the IEEE*, 67(5):786–804, 1979.
- [6] W.A. Heeschen and D.A. Smith. Robust digital image analysis method for counting missing dots in gravure printing. In *Proc. Int. Printing & Graphic Arts Conference*, pages 29–35, Atlanta, GA, USA, 2000.
- [7] Henry R. Kang. *Digital Color Halftoning*. SPIE Press, 1999.
- [8] Anu Langinmaa. An image analysis based method to evaluate gravure paper quality. In *Proc. 11th IAPR Int. Conf. on Computer Vision and Applications*, volume 1, pages 777–780, 1992.
- [9] J.-E. Levlín and L. Söderbjelm. *Pulp and Paper Testing*. Papermaking Science and Technology. Fapet Oy, 1999.
- [10] E. Oja and T. Kohonen. The subspace learning algorithm as a formalism for pattern recognition and neural networks. *IEEE Int. Conf. on Neural Networks*, 1:277–284, 1988.
- [11] P. Piette, V. Morin, and J.P. Maume. Industrial-scale rotogravure printing tests. *Wochenblatt für Papierfabrikation*, 125(16):744–750, 1997.
- [12] Albert Sadovnikov. Automated Heliotest inspection using machine vision. Master’s thesis, Lappeenranta University of Technology, 2003.